

# Effect of Particle Cracking on the Strength and Ductility of Al-SiCp Powder Metallurgy Metal Matrix Composites

Asaad A. Mazen and M.M. Emara

(Submitted 15 May 2002; in revised form 24 July 2003)

The effects of particle cracking on the strength and ductility of Al-SiCp metal matrix composite material (MMC) was investigated. The composite was manufactured using a simple powder metallurgy (PM) technique of hot pressing followed by hot extrusion. Also, the effects of reinforcement weight fraction and strain rate variations on the strength and ductility of the same composite were examined. It was found that particle cracking plays a significant role in controlling the mechanical properties of the composite. It was shown that particle cracking is possible in an MMC material made with a low strength matrix (commercially pure aluminum), and increases with the increase of reinforcement weight fraction, applied strain rate, and amount of plastic deformation. The yield strength increases as a function of reinforcement weight fraction and to a lesser extent as the strain rate increases. The tensile strength increases at low SiCp weight fractions, then remains constant or decreases as more particles are added to the matrix.

**Keywords** ductility, metal matrix composites, particle cracking, powder metallurgy, strain rate, strength

## 1. Introduction

Metal matrix composite materials (MMC) were first developed to respond to a high demand for materials of high strength-to-weight ratio (or high specific strength) and for high-temperature-resistant light materials. Such materials are badly needed for weight-critical applications in the aerospace industry as well as military applications. It is also expected that MMCs will be mass produced to meet the commercial demands for automotive industries. Applications for MMC materials include piston crowns, gudgeon pins, and connecting rods, where the high-temperature strength allows improvements in engine design and operation efficiency.<sup>[1]</sup>

Several techniques of processing are used in manufacturing discontinuously reinforced aluminum (DRA) composites. The most common methods are: casting,<sup>[2,3]</sup> squeeze casting,<sup>[4,5]</sup> vacuum infiltration,<sup>[6,7]</sup> spray deposition techniques,<sup>[8]</sup> and powder metallurgy techniques.<sup>[9]</sup>

Powder metallurgy (PM) techniques have the advantages of uniform distribution of reinforcement in the matrix, finer grain sizes, and better mechanical properties compared with casting methods.<sup>[10]</sup>

Most all of the published work on Al-based MMCs considered a composite with a matrix made up of a high-strength aluminum alloy. Also, processing of the specimens included a degassing or vacuum-pressing step, which adds complication to the processing sequence. McDaniels<sup>[11]</sup> investigated the mechanical behavior of several aluminum MMCs containing up to 40% discontinuous SiC whisker, nodule, or particulate rein-

forcements. The matrices for these composites were made of several aluminum alloys, e.g., 6061, 2024, 7075, etc. Different techniques of manufacturing were used for material fabrication, e.g., PM, direct casting, and hot molding techniques. Davidson<sup>[12]</sup> investigated the tensile deformation and fracture toughness of Al 2014/15 vol% SiC MMC. The material was manufactured using casting followed by hot extrusion at 450 °C with extrusion ratio of 8.2:1. Davies et al.<sup>[13]</sup> investigated the effects of heat treatment on the mechanical behavior and fracture toughness of the 7000 Al-alloys reinforced by different SiCp volume fractions. The material was manufactured by PM techniques of cold compaction in cans, followed by degassing and hot compaction, and finally hot extrusion. Hall et al.<sup>[14]</sup> investigated the effects of particle size, volume fraction, and matrix strength on the fatigue behavior and particle fracture for 2124 aluminum reinforced with SiC particles. PM followed by hot extrusion was used for material manufacturing. Effects of particle size and matrix microstructure were investigated by Lewandowski et al.<sup>[15]</sup> PM techniques were used to fabricate the Al 7xxx composite reinforced by 20 vol% SiC particles of average size 5 or 13  $\mu\text{m}$ , while casting was used to fabricate a 6061 aluminum reinforced by 15 vol%  $\text{Al}_2\text{O}_3$  particles of average size 8-15  $\mu\text{m}$ .

Manoharan and Lewandowski<sup>[16]</sup> studied the effects of microstructure condition, reinforcement size, and reinforcement volume fraction on the fracture initiation and growth in a SiC particulate reinforced 7091 aluminum alloy. They found that nucleation of reinforcement cracking is both matrix and particle size dependent. They also found that while crack initiation toughness showed minor dependence on the size of reinforcement, the crack growth toughness is higher for the composite with larger particle size (13  $\mu\text{m}$ ) compared with that reinforced with smaller particles (5  $\mu\text{m}$ ). Flom and Arsenault<sup>[17]</sup> found that an increase in SiC particle size from 2.4 to 20  $\mu\text{m}$  did not improve the fracture initiation toughness. Kamat et al.<sup>[18]</sup> studied the fracture process in  $\text{Al}_2\text{O}_3$  particulate-reinforced Al-Mg-Cu alloy. They found that the fracture toughness for a rein-

Asaad A. Mazen, Associate Prof., Faculty of Eng., Menia University, Menia, Egypt 61111; and M.M. Emara, Research Engineer, The American University in Cairo, Cairo, Egypt. Contact e-mail: asmazen@msn.com.

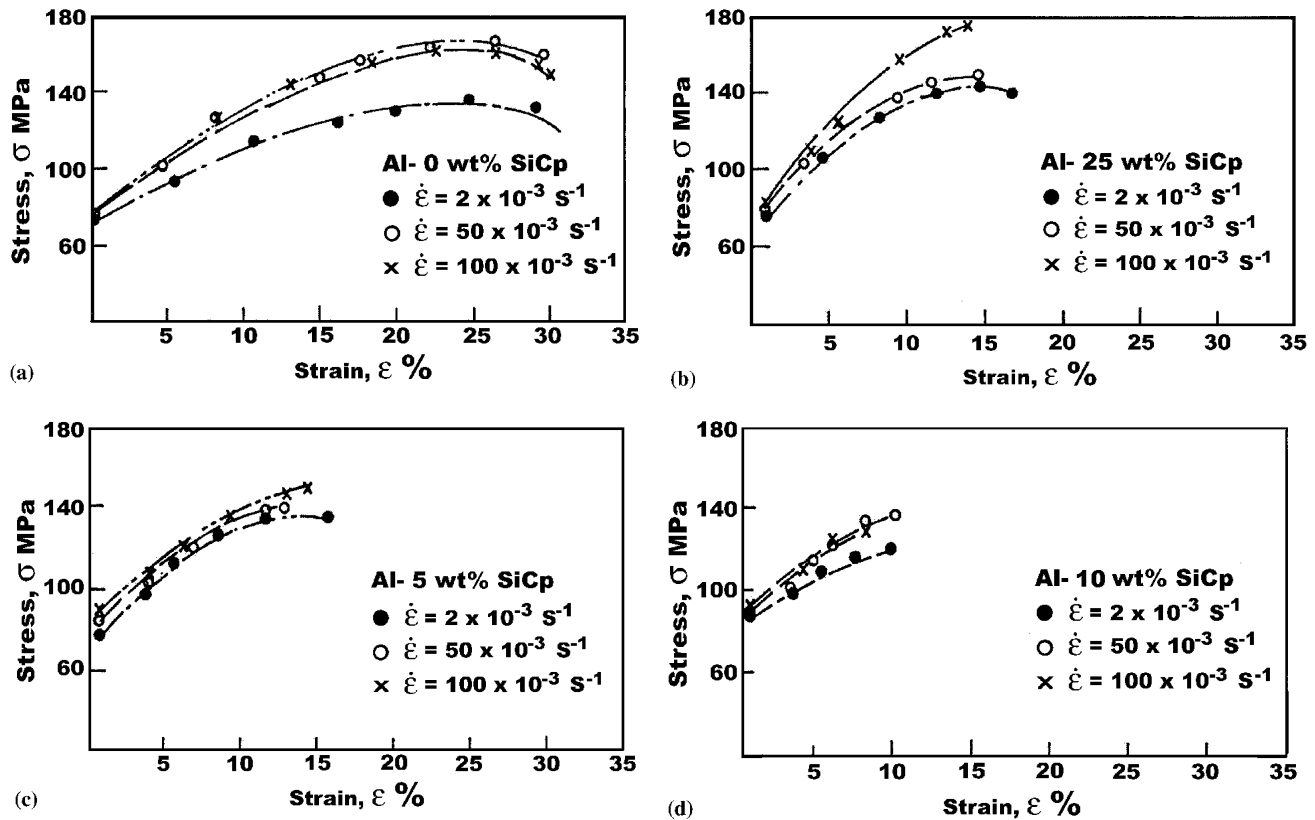


Fig. 1 Tensile plastic stress-strain curves: (a) Al-0 wt.% SiCp, (b) Al-2.5 wt.% SiCp, (c) Al-5 wt.% SiCp, (d) Al-10 wt.% SiCp

Table 1 Porosity in Hot Compacted-Hot Extruded Specimens (a)

Specimen	wt.% SiCp	Porosity % $\pm$ SD (b)
1	0	2.15 $\pm$ 0.128
2	2.5	2.00 $\pm$ 0.174
3	5.0	1.85 $\pm$ 0.614
4	10.0	1.38 $\pm$ 0.289

(a) Based on at least five specimens.  
(b)  $\pm$  Standard deviation.

forcement volume fraction 2-20% increased with interparticle spacing provided that the particle size was less than 15  $\mu\text{m}$ . They concluded that this value correlates with a particle which when cracked presents a microcrack that exceeds the matrix toughness locally.

One of the goals of the present work is to examine particle cracking and its effects in an MMC with low strength matrix. Other goals include investigating the effects of reinforcement weight fraction and variations in applied strain rates on the strength and ductility of this material.

## 2. Experimental Procedures

Prewieghed amounts of aluminum and silicon carbide powders were mixed mechanically to achieve homogeneous distribution of reinforcement particles in the matrix material. The

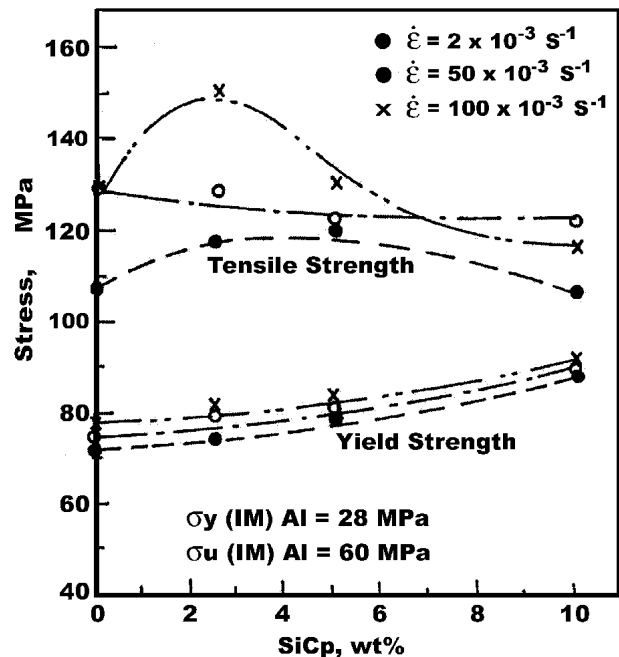


Fig. 2 Variation of yield and tensile strength versus reinforcement weight fraction (see Table 2 for standard deviation values)

average particle size for SiC was 90  $\mu\text{m}$ , and that for aluminum powder was 51  $\mu\text{m}$ . The powders' amounts were precalculated to give the following reinforcement weight fractions: 0, 2.5, 5,

**Table 2 Summary of Mechanical Properties of the Al-SiCp PM MMC at Room Temperature**

Material	Strain Rate $\times 10^{-3} \text{ s}^{-1}$	$\sigma_y$ , MPa (a)	$\sigma_u$ , MPa (b)	% El (c)
Al-0 wt.% SiCp	2	71.80 $\pm$ 1.24 (d)	108.25 $\pm$ 1.10 (d)	31.90 $\pm$ 3.45 (d)
	50	74.60 $\pm$ 3.23	130.40 $\pm$ 3.20	31.10 $\pm$ 3.89
	100	77.02 $\pm$ 0.95	130.40 $\pm$ 1.22	29.60 $\pm$ 4.35
Al-2.5 wt.% SiCp	2	78.29 $\pm$ 1.10	123.70 $\pm$ 5.84	16.70 $\pm$ 2.28
	50	79.30 $\pm$ 1.85	128.20 $\pm$ 1.19	14.60 $\pm$ 1.98
	100	81.55 $\pm$ 3.24	152.50 $\pm$ 8.76	13.60 $\pm$ 1.02
Al-5 wt.% SiCp	2	78.90 $\pm$ 0.54	120.00 $\pm$ 3.25	15.50 $\pm$ 1.24
	50	81.60 $\pm$ 2.26	123.70 $\pm$ 2.59	12.60 $\pm$ 1.73
	100	83.80 $\pm$ 5.40	130.40 $\pm$ 3.69	12.10 $\pm$ 2.20
Al-10 wt.% SiCp	2	88.40 $\pm$ 6.32	108.30 $\pm$ 3.13	10.60 $\pm$ 1.59
	50	90.60 $\pm$ 6.62	123.70 $\pm$ 6.41	9.10 $\pm$ 1.44
	100	90.30 $\pm$ 5.56	117.10 $\pm$ 5.10	8.00 $\pm$ 0.16

(a)  $\sigma_y$ : Yield strength  
(b)  $\sigma_u$ : tensile strength  
(c) % El: Elongation percent to fracture  
(d)  $\pm$  standard deviation

and 10 wt.% SiCp (equivalent to 0, 2.11, 4.22, and 8.5 vol.% SiCp, respectively). The mixtures were fed into a well-lubricated single-acting hard dies for hot compaction. Compaction was accomplished at a temperature of 540 °C, using a pressure of 157 MPa for 3 h. The compact billets were, then, hot extruded at a temperature of 540 °C at an extrusion ratio of 5:1. The extruded billets were machined into test specimens. Porosity in the test specimens was measured using the standard test methods ASTM B328-80.<sup>[19]</sup> The results are shown in Table 1. Tension tests were carried out in an Instron testing machine using average strain rates across the 20 mm gauge length ( $\dot{\epsilon}$ ) of  $2 \times 10^{-3}$ ,  $50 \times 10^{-3}$ , and  $100 \times 10^{-3} \text{ s}^{-1}$  at room temperature. Standard procedures were followed for preparation of specimens for etching and microscopic examination.

### 3. Analysis and Discussion of Results

Figure 1(a)-1(d) show the conventional plastic stress strain curves for the materials under investigation. The curves show the variation of the stress-strain curves with reinforcement weight fraction as a function of the strain rate. Each point on these curves represents the average of at least three test specimens. Table 1 shows a summary of the mechanical properties of the investigated materials at the different testing conditions. The variation of yield and tensile strength of the investigated materials with the applied strain rate is shown in Fig. 3. The yield and tensile strengths (TS) of the ingot metallurgy (IM) aluminum is also indicated on the same figure for comparison.

#### 3.1 Strength and Ductility of Unreinforced Matrix

Figure 1(a) shows the tensile deformation behavior of the unreinforced matrix (Al-0 wt.% SiCp) processed by the present PM technique. It can be seen that considerable improvements in strength as well as ductility have been achieved compared with pure aluminum processed by IM. The unreinforced PM aluminum of the current study showed yield strength of about 79 MPa, and a true maximum stress of 136.15 MPa (corre-

sponding to a conventional tensile strength of 108.25 MPa) at an average strain rate of  $2 \times 10^{-3} \text{ s}^{-1}$ . At strain rates ( $\dot{\epsilon}$ ) of  $50 \times 10^{-3}$  and  $100 \times 10^{-3} \text{ s}^{-1}$ , the true maximum strength of the material rose to 161.3 and 164.2 MPa, respectively. IM processed pure aluminum has yield and tensile strengths of about 28 and 60 MPa, respectively.<sup>[20]</sup> Thus, the present technique achieved an improvement in yield strength of about 282% and in tensile strength of about 268-273% of the IM values.

The ductility of unreinforced matrix was evaluated using the percent elongation to fracture (%El.). No necking was observed in any of the tested specimens, which justifies the use of %El as a measure of ductility. It was found that the %El. = 31.9% at  $\dot{\epsilon} = 2 \times 10^{-3} \text{ s}^{-1}$ . Such value is comparable to the values achieved in IM processed pure aluminum.<sup>[20]</sup> Thus, the present technique did not cause significant reduction in the material ductility like other techniques, e.g., casting. The increase in applied strain rate caused a corresponding increase in both the yield strength and tensile strength of the unreinforced matrix. At a strain rate of  $100 \times 10^{-3} \text{ s}^{-1}$ , the yield strength increased by 7.2% compared with its value at  $\dot{\epsilon} = 2 \times 10^{-3} \text{ s}^{-1}$ . On the other hand, the tensile strength of the unreinforced matrix at  $\dot{\epsilon} = 100 \times 10^{-3} \text{ s}^{-1}$  increased by 20.5% compared with its value at  $\dot{\epsilon} = 2 \times 10^{-3} \text{ s}^{-1}$ .

The strain rate variations slightly affected the ductility of the unreinforced matrix. As  $\dot{\epsilon}$  increased, the ductility of Al-0 wt.% SiCp decreased from 31.9% to 29.6%.

#### 3.2 Effects of Reinforcement Weight Fraction and Strain Rate Variations on the Strength of Al-SiCp MMC

Figure 1(b)-1(d) show the plastic stress strain curves of the different compositions of the Al-SiCp MMC. It can be seen that introducing hard and brittle SiC particles into the soft pure aluminum matrix lead to improvement in the yield strength of this matrix. This can also be seen in Fig. 2, which plots the variation of yield strength versus SiCp weight fraction as a function of the applied strain rate. Compared with the unreinforced matrix, the yield strength of the composite achieved an

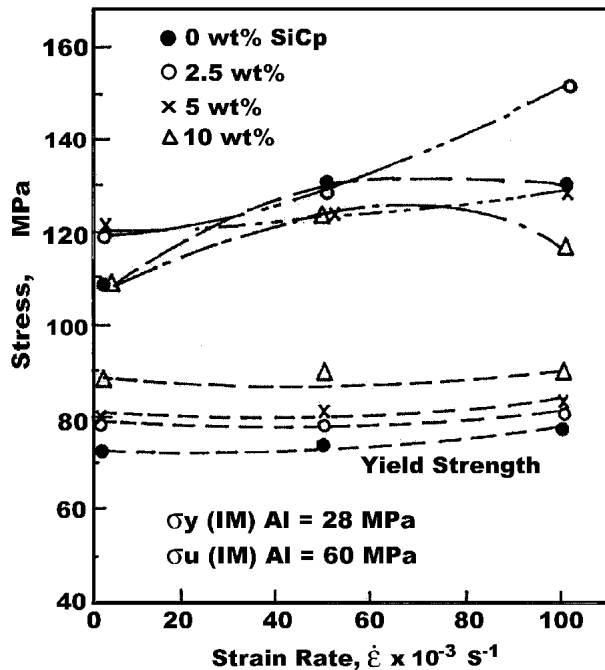


Fig. 3 Variation of yield and tensile strength versus strain rate

improvement of 9% at 2.5 wt.% SiCp, 9.8% at 5 wt.% SiCp, and 23.2% at 10 wt.% SiCp. Compared with ingot metallurgy (IM) pure aluminum, these improvements are 279%, 279%, and 315%, respectively. It can be seen from Fig. 3 that the increase in yield strengths with the strain rates is not as significant as it is with the reinforcement weight fraction. Thus, it may be concluded that the yield strength of Al-SiCp PM MMC is not strain rate sensitive within the range of reinforcement weight fractions investigated at room temperature. This depicts a matrix-controlled behavior.

From both Fig. 2 and 3, it can be seen that, for each applied strain rate, the tensile strength (TS) improves for the lowest amount of SiCp weight fraction added to the unreinforced matrix. Then, as more SiC particles are added, the tensile strength levels off or decreases. For example, at a strain rate of  $2 \times 10^{-3} \text{ s}^{-1}$ , the Al-0 wt.% SiCp had a TS = 108.2 MPa, which increased up to 119.7 MPa for Al-2.5 wt.% SiCp, and remained almost the same (120 MPa) at 5 wt.% SiCp, then decreased to 108.3 MPa at 10 wt.% SiCp. On the other hand, as the strain rate increased, the tensile strength increased for all reinforcement weight fractions. For example, the TS of Al-5 wt.% SiCp increased by 8.6% and that of Al-10 wt.% SiCp increased by 8.12% as the strain rate increased from  $2 \times 10^{-3} \text{ s}^{-1}$  to  $100 \times 10^{-3} \text{ s}^{-1}$  in each case. The Al-2.5 wt.% SiCp showed a significant increase by about 27.4% as the strain rate increased from  $2 \times 10^{-3} \text{ s}^{-1}$  to  $100 \times 10^{-3} \text{ s}^{-1}$ .

### 3.3 Effects of Reinforcement Weight Fraction and Strain Rate on Ductility of Al-SiCp MMC

The effects of reinforcement weight fraction and strain rate variations on the ductility of Al-SiCp PM MMC are shown in Table 1 and Fig. 4. It can be seen that the ductility (measured

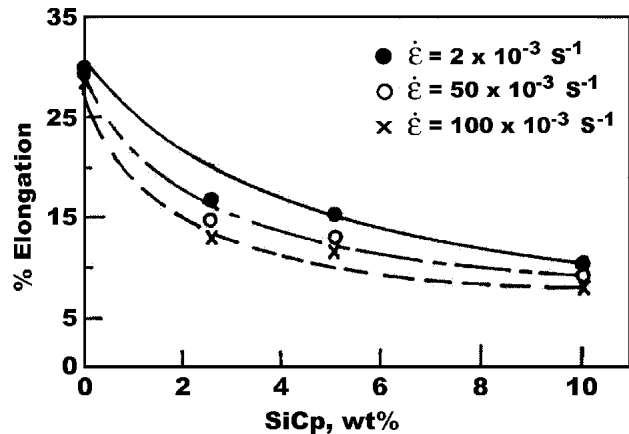


Fig. 4 Effects reinforcement weight fraction and strain rate variations on ductility

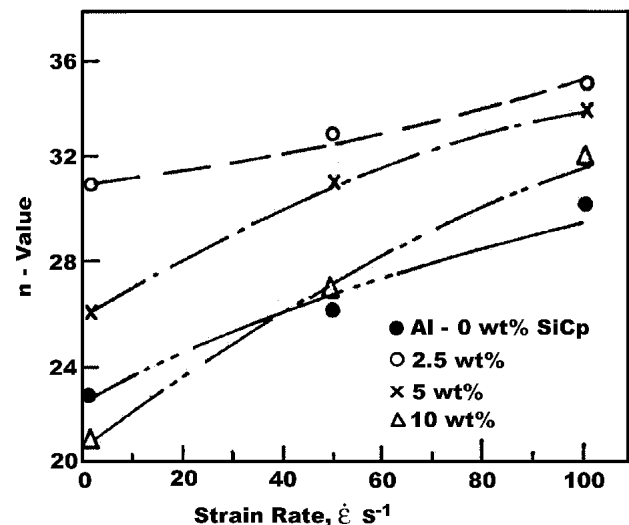


Fig. 5 Effects of reinforcement weight fraction and strain rate variations on the hardening behavior

by the %El) decreased as the reinforcement weight fraction increased and as the applied strain rate increased. However, it seems that the reinforcement weight fraction has greater negative effect on the ductility than the increase in strain rate. For example: the ductility decreased from 16.7% for Al-2.5 wt.% SiCp at  $\dot{\epsilon} = 2 \times 10^{-3} \text{ s}^{-1}$  to 10.6% for Al-10 wt.% SiCp, at the same strain rate, i.e., a reduction of about 36%. On the other hand, the ductility of Al-2.5 wt.% SiCp decreased from 16.7% at  $\dot{\epsilon} = 2 \times 10^{-3} \text{ s}^{-1}$  to 13.6% at  $\dot{\epsilon} = 100 \times 10^{-3} \text{ s}^{-1}$ , i.e., a reduction of about 18.5%. Similar behavior was exhibited by the other reinforcement weight fractions.

### 3.4 Effects of Reinforcement Weight Fraction and Strain Rate Variations on the Work-Hardening Behavior

The work-hardening behavior was evaluated by calculating the work-hardening exponents  $n$ , in the simple power law  $\sigma = k\epsilon^n$ , where  $\sigma$ ,  $\epsilon$ , and  $k$ , are true stress, true strain, and material

strength coefficient, respectively. The effects of reinforcement weight fraction and strain rate variations are shown in Fig. 5. It can be seen that for any reinforcement weight fraction, the higher the applied strain rate the higher the work-hardening exponent. On the other hand, the work-hardening exponent increased at the lowest SiCp weight fraction (2.5 wt.%), then decreased as more SiCp weight fractions were added to the matrix. This trend resembles that of the variation of tensile strength with reinforcement weight fractions (see Fig. 2). This is a matrix-controlled behavior. It can be explained according to the known mechanism of hardening due to lack of time for dislocation rearrangement and slip.<sup>[21]</sup>

### 3.5 Effects of Particle Cracking

The yield strength of the Al-SiCp MMC of the present work improved as a function of reinforcement weight fraction. This

improvement could be attributed to the dislocation mechanisms of strengthening. These mechanisms were summarized in Ref. 22 as dislocation generation and entanglement due to plastic work and thermal mismatch (which is evident during hot compaction and hot extrusion followed by cooling in air), the Orowan mechanism, grain size strengthening, and formation of dislocation cell structure around reinforcement particles.

The TS, on the other hand, showed an increase in its magnitude at low SiCp weight fractions followed by a decrease or at best remained constant at higher weight fractions. Once plastic deformation begins, the flow stress of the material becomes the resultant of two opposing mechanisms: the strengthening mechanisms mentioned above, and softening mechanisms which act to ease the plastic flow and reduce the strength of the material. The presence of hard particles leads to geometric softening in the material by interruption of dislocation

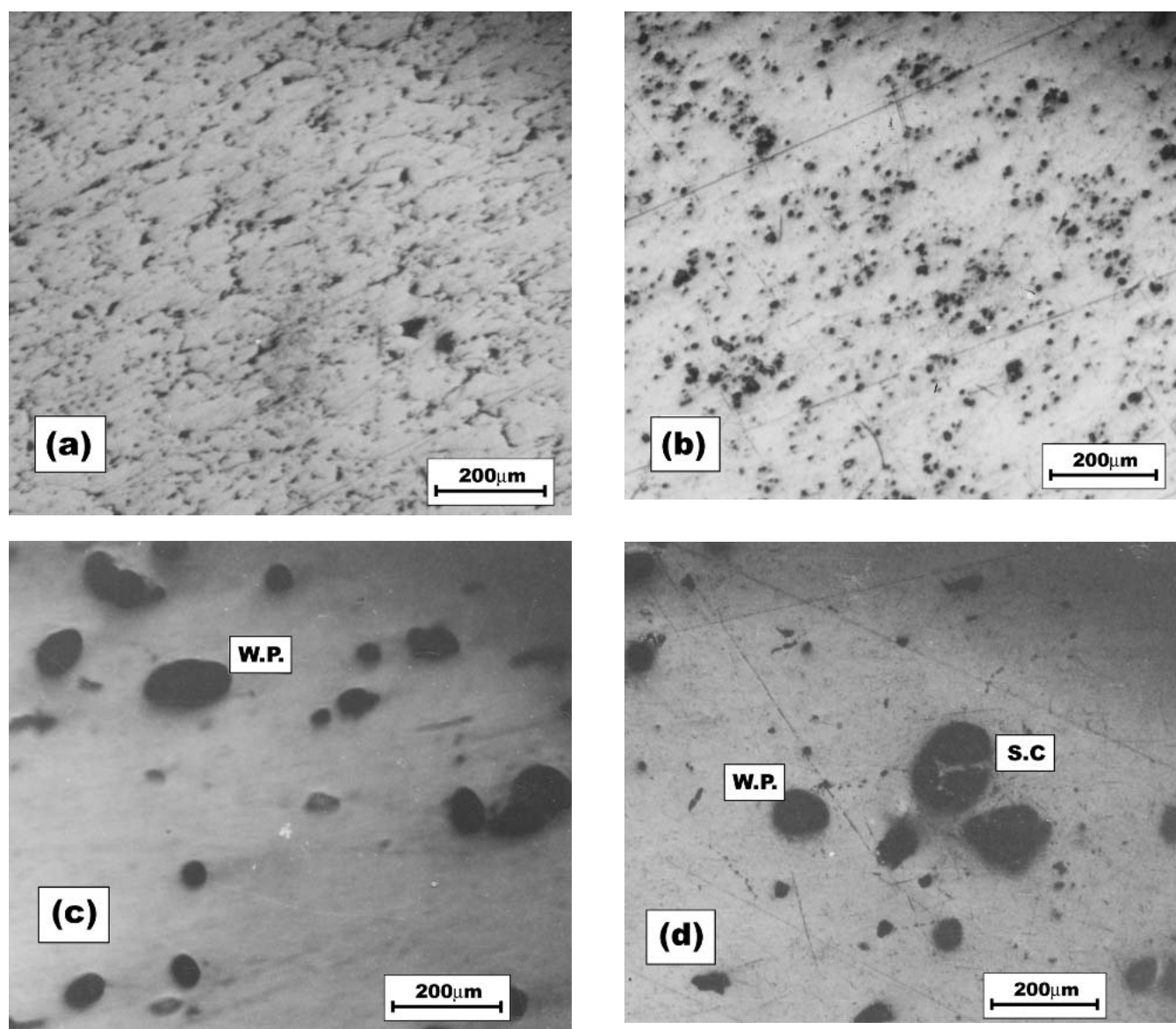


**Fig. 6** Micrographs showing particle cracking: (a) Al-0 wt.% SiCp before deformation, (b) Al-0 wt.% SiCp after deformation, (c) Al-2.5 wt.% SiCp heavily etched, before deformation, (d) Al-2.5 wt.% SiCp heavily etched, after deformation

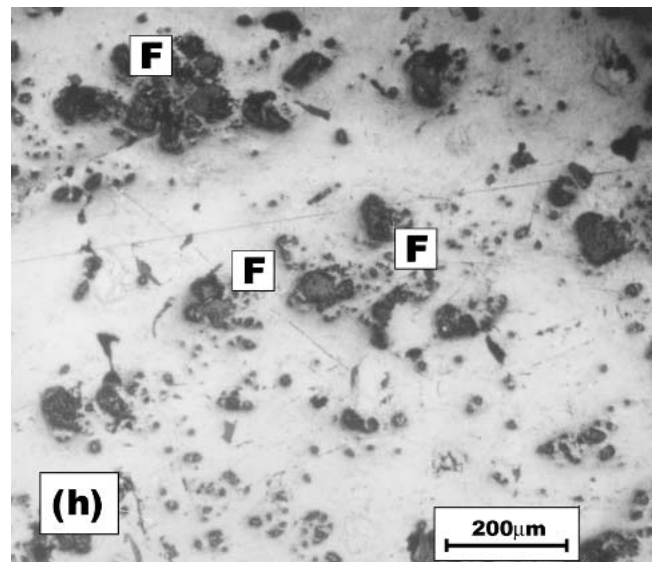
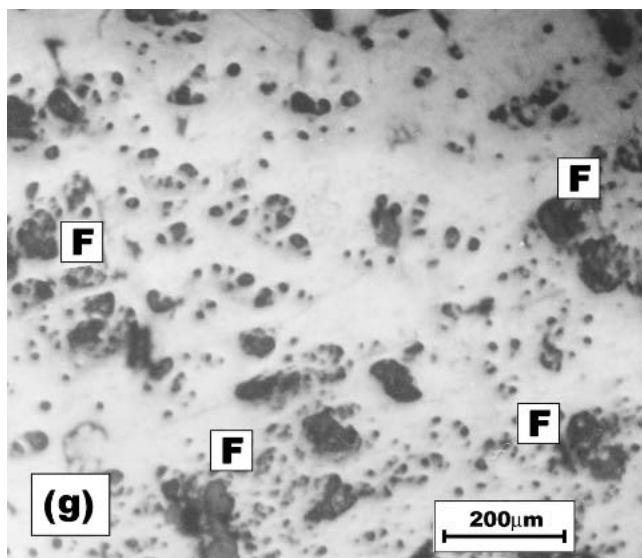
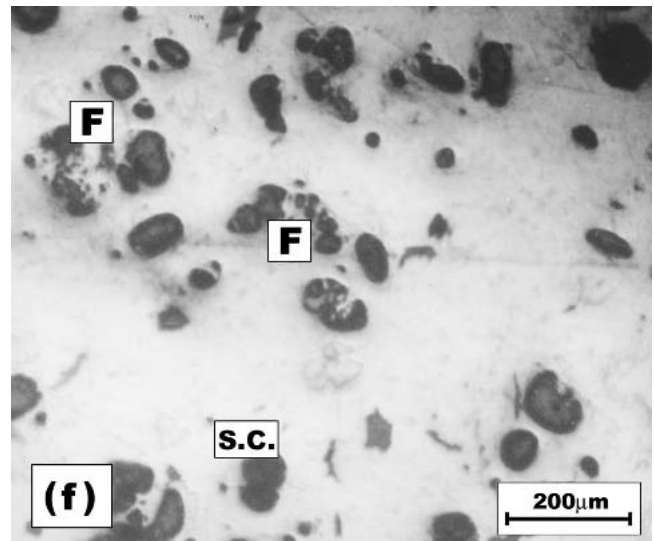
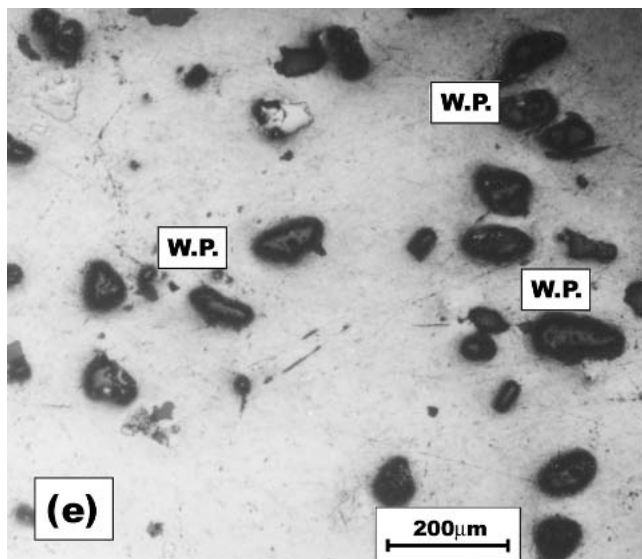


**Fig. 6 cont.** Micrographs showing particle cracking: (e) Al-5 wt.% SiCp before deformation (heavily etched), (f) Al-5 wt.% SiCp after deformation (heavily etched), (g) Al-10 wt.% SiCp (deformed up to fracture at low strain rate, heavily etched), (h) Al-10 wt.% SiCp (deformed up to a plastic strain of 2% at high strain rate, heavily etched) (W.P.: Whole particle, S.C.: Single crack, F: Fragmentation).

glide providing an outlet for these moving dislocations preventing them from piling-up and entanglements. Stress concentration due to reinforcement particles is another source that accelerates the microscopic deformation causing void nucleation and reduction in the deformation process (this remark is in good agreement with the deformation behavior shown in Fig. 1a-d). Levy and Papazian<sup>[23]</sup> conducted a finite element analysis of MMC materials, which showed that the local stress could reach a maximum in the matrix near the particles. McDaniels<sup>[11]</sup> attributed the reduction in strength of the MMC with high volume fraction (30-40 vol% SiC) to the disability of the matrix to redistribute the internal stresses due to lack of enough ductility, which is in agreement with the explanation given above. Manoharan and Lewandowski<sup>[16]</sup> suggested that the load transferred from the matrix to the particles might ex-

ceed the particle strength-causing particle cracking, which becomes another source of stress concentration and strength and ductility reduction. They suggested that such mechanism could take place only in MMCs with high strength matrices.

To examine this point for an MMC with a low strength matrix, like the one used in the present work, several sections were taken and examined in an optical microscope from undeformed specimens, and deformed specimens. Heavy etching was used to reveal the particles by matrix dissolution in the HF + HCl etchant.

Figure 6(a) and 6(b) show micrographs of etched specimens of unreinforced aluminum (Al-0 wt.% SiCp) before and after deformation, respectively. It can be seen that the residual porosity retained during processing (Fig. 6a) opened-up as a result of tensile deformation (Fig. 6b).

**Table 3 Percentage of Particles Cracked by Single Crack and by Fragmentation for Each Set of Testing Conditions**

Micrograph	Material	$\dot{\epsilon} \times 10^{-3} \text{ s}^{-1}$ (a)	$\epsilon_D$ , % (b)	% of Particles Cracked $\pm$ SD (c)		Remarks
				Single Crack	Fragmentation	
Fig. 6(a)	Al-0 wt.% SiCp	...	...	...	...	Residual porosity
Fig. 6(b)	Al-0 wt.% SiCp	2.0	30 (F)(d)	...	...	Porosity opened-up
Fig. 6(c)	Al-2.5 wt.% SiCp	...	...	...	...	Particles are intact
Fig. 6(d)	Al-2.5 wt.% SiCp	100	29 (F)	$12 \pm 1.70$	...	Single cracked particles
Fig. 6(e)	Al-5 wt.% SiCp	...	...	...	...	Particles are intact
Fig. 6(f)	Al-5 wt.% SiCp	2.0	15 (F)	$9 \pm 2.9$	$5 \pm 1.34$	Cracking and fragmentation
Fig. 6(g)	Al-10 wt.% SiCp	2.0	10 (F)	$5.7 \pm 1.90$	$70 \pm 3.71$	Extensive cracking and fragmentation
Fig. 6(h)	Al-10 wt.% SiCp	100	2.0	$8.0 \pm 2.02$	$60 \pm 2.92$	Extensive cracking and fragmentation

(a)  $\dot{\epsilon}$ : Strain rate

(b) Global plastic strain

(c)  $\pm$  SD:  $\pm$  standard deviation

(d) (F): Fracture strain

Results are based on at least five specimens.

Figure 6(c) and 6(d) show micrographs of heavily etched specimens of Al-2.5 wt.% SiCp before and after tensile deformation, respectively. It can be seen that before deformation (Fig. 6c) the particles are intact and undamaged. After deformation at high strain rate ( $100 \times 10^{-3} \text{ s}^{-1}$ ) up to fracture, some particles cracked with a single crack.

Figure 6(e) and 6(f) show micrographs of healthy etched specimens of Al-5 wt.% SiCp before and after deformation. Again, before deformations the particles are intact and undamaged, while after deformation, at low strain rate ( $2 \times 10^{-3} \text{ s}^{-1}$ ) up to fracture, particle cracking, and some fragmentation are clear, but not extensive.

Figure 6(g) and 6(h) show micrographs of heavily etched specimens of Al-10 wt.% SiCp after tensile deformation at low strain rate up to fracture, and at high strain rate up to a low strain of 2%, respectively. Extensive particle cracking and fragmentation can be seen in both micrographs.

Table 3 summarizes these findings and gives the percentages of particles cracked by a single crack and by fragmentation for each set of testing conditions.

These microscopic results show that particle cracking is possible in MMCs with low strength matrices as it is in MMCs with high strength ones. They also show that the factors controlling such damage are: reinforcement weight fraction, amount of plastic strain, and strain rate.

From Fig. 1(a)-1(d), and the micrographs Fig. 6(a)-6(h), it seems that particle cracking has little effect on the yield strength but has a significant effect on the TS. This should be expected in view of the fact pointed above; i.e., particle damage is plastic strain dependent.

Ductility of all specimens was shown to decrease as the reinforcement weight fraction increased and as the strain rate increased (see Table 1). This seems to be in agreement with the microscopic results shown above. It also shows that particle cracking is a major factor in controlling the ductility of particulate MMCs.

## 4. Conclusions

Based on the current study, the following conclusions can be drawn:

- Particle cracking is possible in MMC's with low strength matrices. It depends on reinforcement weight fraction, the applied strain rate, and the amount of plastic strain. Particle cracking plays a major role in controlling the strength and ductility of MMCs.
- The yield strength of the aluminum matrix increases as more reinforcement particles are added and as the applied strain rate increases. However, the latter has lesser effect than the former.
- The tensile strength of Al-SiCp MMC of the present work improves at the lowest SiCp weight fraction, then remains constant or decreases as more particles are added. This was shown to be related to particle damage during plastic deformation or due to the increase in strain rate.
- The ductility of the present Al-SiCp MMC decreases as more SiCp are added to the matrix and at higher strain rates. However, SiCp weight fraction has more negative effect on ductility than strain rates.
- The hardening behavior of the present MMC was shown to be matrix controlled; i.e., the work-hardening exponent  $n$  increases with the increase in applied strain rate.

## References

1. A.L. Geiger and J.A. Walker: "Advances in Metal Matrix Composites," *J. Metals*, 1991, 43, p. 8.
2. A.W. Urquhart: "Molten Metal MMC and CMC's," *Adv. Mater. Proc.*, 1991, 7, p. 25.
3. M.K. Aghajanian, M.A. Rocazella, J.T. Burke, and S.D. Keck, "Fabrication of Mmc By A Pressureless Infiltration Technique," *J. Mater. Sci.*, 1991, 26, p. 447.
4. T.W. Clyne and P.J. Withers, *An Introduction to Metal Matrix Composites*, Cambridge Univ. Press, Cambridge, UK, 1995.
5. M.G. McKimpson, and T.E. Scott: "Processing and Properties of MMC Containing Discontinuous Reinforcement," *Mater. Sci. Eng.*, 1989, A 107, pp. 93-106.
6. J.-Yang and D.D.L. Chung: "Casting Particulate and Fibrous MMC by Vacuum Infiltration of a Liquid Metal under Inert Gas Pressure," *J. Mater. Sci.*, 1989, 24, p. 3605.
7. J.M. Chiou and D.D.L. Chung, "Characterization of MMC Fabricated by Vacuum Infiltration of a Liquid Metal under Inert Gas Pressure," *J. Mater. Sci.*, 1991, 26, p. 2583.
8. E.J. Lavernia, "Spray Atomized and Codeposited 6061 Al/SiC Composites," *SAMPE Quarterly*, 1991, 22(2), pp. 2-12.
9. Y.B. Lui, S.C. Lim, L. Lu, and M.O. Lai: "Recent Development in

- the Fabrication of Metal Matrix-Particulate Composites Using Powder Metallurgy Techniques," *J. Mater. Sci.*, 1994, 29, p. 1999.
10. I.A. Ibrahim, F.A. Mohamed, and E.J. Lavernia: "Particulate Reinforced MMC—A Review," *J. Mater. Sci.*, 1991, 26, p. 1137.
  11. D.L. McDaniels, "Analysis of Stress-Strain, Fracture, and Ductility Behavior of Aluminum Matrix Composites Containing Discontinuous SiC Reinforcement," *Metall. Trans. A*, 1985, 16A, p. 1105.
  12. D.L. Davidson: "Tensile Deformation and Fracture Toughness of 2014+15Vol. Pct. SiC Particulate Composite," *Metall. Trans. A*, 1991, 22A, p. 113.
  13. C.H.J. Davies, N. Raughunathan, and T. Sheppard: "Structure-Property Relationships of SiC Reinforced Advanced Al-Zn-Mg-Cu Alloy," *Mater. Sci. Technol.*, 1992, 8, p. 977.
  14. J.N. Hall, J.W. Jones, and A.K. Sachdev: *Mater. Sci. Eng.*, 1994, A 183, p. 69.
  15. J.J. Lewandowski, D.S. Liu, and C. Liu: *Script. Metall. Mater.*, 1991, 25, p. 21.
  16. M. Manoharan and J.J. Lewandowski: "Effect of Reinforcement Size and Matrix Microstructure on the Fracture Properties of an Al-MMC," *Mater. Sci. Eng.*, 1992, A 150, p. 179.
  17. Y. Flom and R.J. Arsenault: *Acta Metall.*, 1989, 37, p. 2413.
  18. S.V. Kamat, J.P. Hirth, and R. Mehrabian: "Work Hardening Behavior of Alumina Particulate Reinforced 2024 Aluminum Alloy MMC," *Acta Metall.*, 1989, 37, p. 2395.
  19. Anon.: ASTM-B328, *Annual Book of ASTM Standards*, ASTM, Philadelphia, PA, 1980.
  20. W.D. Callister, Jr., *Materials Science and Engineering*, John Wiley & Sons, New York, 1989, p. 95.
  21. D. Lee and D.A. Woodford, in *The Inhomogeneity of Plastic Deformation*, American Society for Metals, Metals Park, OH, 1973, p. 114.
  22. W.S. Miller and F.J. Humphreys, "Strengthening-Mechanisms in Particulate MMC," *Scripta Metall. Mater.*, 1991, 25, p. 33.
  23. A. Levy and J.M. Papazian, "Tensile Properties of Short Fiber Reinforced SiC/Al Composites: Part II. Finite Element Analysis," *Metall. Trans A*, 21A, 1990, p. 411.